Macromolecules
ARTICLE

Macromolecules **2009**, *42*, 6253–6260 **6253**
DOI: 10.1021/ma900925q

Chiral Micelles of Achiral TPPS and Diblock Copolymer Induced by Amino Acids

Lizhi Zhao, Xin Wang, Yan Li, Rujiang Ma, Yingli An, and Linqi Shi*

Key Laboratory of Functional Polymer Materials, Ministry of Education, and Institute of Polymer Chemistry, Nankai University, Tianjin 300071, China

Received April 28, 2009; Revised Manuscript Received July 9, 2009

ABSTRACT: Chiral complex micelles prepared by 5,10,15,20-tetrakis(4-sulfonatophenyl)porphyrin (TPPS) and the poly(ethylene glycol)-*block*-poly(4-vinylpyridine) (PEG_{114}-*b*-$P4VP_{61}$) in the presence of aspartic acid (Asp), tryptophan (Trp), and lysine (Lys) were investigated in aqueous solutions at pH 2.0. TPPS formed J-aggregates in the micellar core. The morphology and optical properties of the complex micelles depended on the properties of amino acids and the preservation time for the mixed solutions of TPPS and amino acids before adding the copolymer. Prolonging the preservation time, the spherical morphology of the complex micelles remained unchanged in the presence of the Asp. On the contrary, a morphology evolution from sphere to rod took place for Trp and Lys. The intensity of the circular dichroism (CD) signals of the complex micelles increase with the preservation time, and the chirality sign was determined by amino acids. L-Trp and L-Lys led to a negative chirality sign and L-Asp a positive one while the corresponding enantiomers contributed to the opposite sign. Lower concentration of amino acids could not transfer their chirality to the aggregates of TPPS, and at higher concentrations of TPPS, it took more time for the aggregates to express the chiral information on amino acids.

Introduction

The chirality of molecules and supramolecular systems has attracted extensive interest of researchers because of its essential role in life and material sciences.[1−4] Supramolecular chirality is usually achieved by noncovalent interaction. It can be obtained not only from chiral molecules but also from achiral molecules induced by chiral template.[5,6] Besides, a physical force in the symmetrical breakage of aggregates formed by absolute achiral molecules is of great importance in the fabrication of supramolecular chirality systems.[7] In polymer science, supramolecular chirality can be expressed by the helical conformation of polymer chains and the tertiary structures formed by a self-assembly of chiral polymers.[8−11] The supramolecular chirality formation, which is ubiquitous in nature, becomes the candidates for other applications, such as asymmetric catalysis and autocatalysis,[12] nonlinear optics,[13] molecular recognition and self-assembly,[14] and in molecular device design.[15] In addition, this phenomenon has been proved a useful tool in the determination of the absolute configuration of chiral compounds.[16]

Water-soluble porphyrins are well-investigated dyes due to their special structural, optical, and electrical properties and the applications in medicine and materials chemistry.[17] They are also widely used in chiral supramolecular systems. Purrello et al. have investigated the processes concerning the transfer and storing of chiral information from chiral polymer or noncovalent polymer templates to achiral porphyrin.[18] Ribo et al. have studied the effect of vortex motion and stirring on the chirality formation of porphyrin.[19,20] A series of works have been carried out by Liu's group involving the induced chirality of porphyrin on the chiral films[21] and at the air/water interface.[22] 5,10,15,20-Tetrakis-(4-sulfonatophenyl)porphyrin (TPPS) possessing zwitterionic character has been the focus of extensive studies because it can form highly ordered molecular J- and H-aggregates under certain concentration, pH value, and ionic strength.[23−25] Furthermore, polycations are highly efficient in inducing the aggregation.[26]

Amphiphilic block copolymers with controlled architectures, narrow molecular weight distributions, and well-defined molecular weights are apt to self-assemble into micelles in a selective solvent, which makes them act as macromolecular surfactants. Such polymeric micelles have the potential applications as nanoreactors, drug and gene delivery devices, and structure directive templates.[27−29] We have recently reported that TPPS and poly(ethylene glycol)-*block*-poly(4-vinylpyridine) (PEG-*b*-P4VP) were able to form micelles based on their electrostatic interaction with J-aggregation of TPPS in the micelle core.[30,31] PEG-*b*-P4VP here is a typical double hydrophilic block copolymer (DHBC) bearing the pH-responsive block P4VP, which turns into a polycations at pH below its pK_a. Varying the ratio of the cationic units of PEG-*b*-P4VP to the sulfonate groups of TPPS or dialyzing against more acidic aqueous solutions endowed the complex micelles with a chirality property. The chiral complex micelles may have novel applications in chiral separation, asymmetrical catalysis, molecular recognition, entrapment, and release of drugs.

In this paper, we further discuss the supramolecular chirality in the polymeric micelle system. Three α-amino acids were chosen as the chiral template: aspartic acid (Asp), the acidic species possessing an excessive carboxyl group, lysine (Lys), the basic species with an excessive amino group, and tryptophan (Trp). The properties of the small chiral molecules determine the chirality sign of the micellar systems, and the morphology of the complex micelles depends on the preservation time for TPPS solutions with the amino acids. The optical properties were investigated with the aid of a circular dichroism and UV−vis spectrophotometer. Dynamic light scattering and atomic force microscope were used to characterize the resulting complex micelles.

*Corresponding author: Tel 86-22-23506103, Fax 86-22-23503510, e-mail shilinqi@nankai.edu.cn.

Published on Web 07/27/2009

Experimental Section

Materials. 5,10,15,20-Tetrakis(4-sulfonatophenyl)porphyrin (TPPS) was purchased from Dojindo Laboratories as an acid and used without further purification. L-(or D-)tryptophan, L-(or D-)aspartic acid, and L-(or D-)lysine were purchased from Alfa Aesar and used as received. The block copolymer PEG_{114}-*b*-$P4VP_{61}$ was synthesized by atom transfer radical polymerization (ATRP).[32] The composition of the block copolymer was characterized by ^1H NMR spectrum in $CDCl_3$ using the PEG blocks as the inner standard. The polydispersity index (M_w/M_n) of the block copolymer was characterized to be 1.15 by gel permeation chromatography (GPC) using *N*,*N*-dimethylformamide (DMF) as the eluent and narrowly distributed poly(methyl methacrylate) as the calibration standard.

Preparation of the TPPS/PEG_{114}-*b*-$P4VP_{61}$ Complexes. The method for preparation of the TPPS/PEG_{114}-*b*-$P4VP_{61}$ complexes was described as follows. First, the TPPS solution was prepared by dissolving in the neutral Milli-Q water (18 MΩ), stored in the dark, and used within a day after preparation. The concentration of the TPPS solution (40 μmol/L) was determined spectrophotometrically using $\varepsilon_{414} = 5.33 \times 10^5$ L/(mol cm) at the Soret maximum from an aliquot of the stock solution diluted 1/20 by volume with 0.1 mM phosphate buffer.[33] The block copolymer PEG_{114}-*b*-$P4VP_{61}$ and the amino acids L-(or D-) tryptophan, L-(or D-)aspartic acid, and L-(or D-)lysine) were dissolved in acidic aqueous solution at pH 2 (adjusted by hydrochloric acid and no buffer was used). The concentration of the polymer stock solution was 0.5 g/L, and those of the amino acids stock solutions were 40 mmol/L. Next, the micellization was carried out by adding certain volume of the TPPS stock solutions into the diluted amino acid solutions, and then the mixed solutions were stored for several hours before adding the polymer solution.

Atomic Force Microscopy (AFM). The complex micelles were imaged using a tapping mode AFM (Veeco Company, Multimode, Nano IIIa). The samples for AFM measurements were prepared by casting a droplet (20−50 μL) of the micelle solution onto a basal plane of micaceous substrate. The solution was then blotted off with the tip of a filter paper after 10 s. The sample was finally dried in a vacuum desiccator for a week.

Transmission Electron Microscopy (TEM). TEM measurements were performed with a commercial Philips T20ST electron microscope at an acceleration voltage of 200 kV. To prepare the TEM samples, a small drop of the solutions was deposited onto the carbon-coated copper electron microscopy (EM) grid and then dried under room temperature and atmospheric pressure.

Light Scattering (LS). The micelle solutions for DLS (dynamic light scattering) analysis were prepared by filtering samples (about 1 mL) through a 0.45 μm Millipore filter into a clean scintillation vial. For TPPS and amino acids mixed solutions, there were a few differences from the micelle solutions in the manipulation. Practically, 1 mL of acidic aqueous solutions at pH 2 with and without the three kinds of amino acids was filtered into the scintillation vials, and then a small quantity of filtered stock TPPS solutions was added. The measurements were carried out immediately to attain the data within 4−5 min elapsed time. Another measurement on the time history of the scattered light intensity was carried out to track the aggregation process of TPPS after the mixing. The procedures were performed on a laser light scattering spectrometer (BI-200SM) equipped with a digital correlator (BI-10000AT) at 532 nm at 20 °C.

Other Characterization Techniques and Measurements. UV−vis absorption spectra were measured on a TU-1810 UV−vis spectrophotometer (Purkinje General, China) at 20 °C. Circular dichroism (CD) spectra were recorded at room temperature by a Hitachi Jasco-J710 circular dichroism spectrophotometer (Japan).

Results and Discussion

Fabrication of the TPPS/PEG_{114}-*b*-$P4VP_{61}$ Complex Micelles and J-Aggregation of TPPS in the Presence of Amino Acids. TPPS is water-soluble and exists as a monomer at the concentrations below 50 μM. The absorption spectra of the deprotonated species (pK_a 4.9), H_2TPPS^{4-}, exhibit features of D_{2h} symmetry. At low pH, nitrogens in the macrocycle of the ionic porphyrin are protonated (H_4TPPS^{2-}), and symmetry increases to D_{4h} with a shift of the Soret band from 413 to 434 nm and a decrease in the number of Q bands from four to two because of the degeneracy of the excited state.[34] Under more acidic conditions, two new absorption bands may appear at about 490 and about 706 nm, which are assigned to the formation of J-aggregates.

In acidic aqueous solution, the PEG_{114}-*b*-$P4VP_{61}$ transforms into a typical neutral−cationic double hydrophilic block copolymer (DHBC) due to protonation of the P4VP blocks (pK_a 4.5−4.7).[35] Scheme 1 shows the molecular structures of TPPS and PEG_{114}-*b*-$P4VP_{61}$.

Thus, the micellization of the block copolymer in the presence of TPPS takes place easily because of the electrostatic attraction between the $4VPH^+$ units of PEG_{114}-*b*-$P4VP_{61}$ and the $-SO_3^-$ groups of the TPPS and results in a promoted aggregation of TPPS at low pH values.[31] However, the presence of amino acids also leads to self-assembly of TPPS. Table 1 summarizes the intensity-weighted CONTIN analysis of TPPS aggregates in the absence and presence of Asp, Trp, and Lys in comparison with that of complex micelles at the scattering angle of 90°. Of particular manipulation, in the case of TPPS aggregates, the measurements

Scheme 1. Structures of the Diacid (H_4TPPS^{2-}) and Free-Base (H_2TPPS^{4-}) Forms of the Tetrakis(4-sulfonatophenyl)porphrin and PEG_{114}-*b*-$P4VP_{61}$

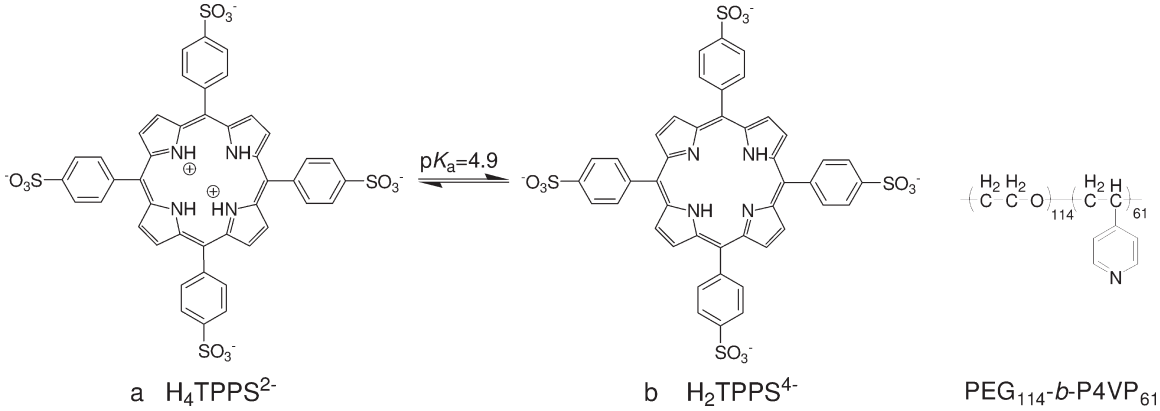

Table 1. Hydrodynamic Diameters of TPPS Aggregates and the Complex Micelles in the Presence of Amino Acids

D_h/nm	pure TPPS	Asp	Trp	Lys
TPPS aggregates				
small	39.7	28.5	56.2	116.4
large	426.6	398.2	562.3	645.5
complex micelles	102.1	104.0	112.8	157.0

were started as soon as the samples were prepared, and the results were all obtained within 4−5 min elapsed time to compare the diameters of initial stage. The diameters are bimodal distributed as shown in Figure S1, which are centered at 39.7, 426.6 nm for pure TPPS, indicating the coexistence of small and large aggregates. Similarly in the presence of amino acids, bimodal size distributions can also be detected centered at 28.5, 398.2 nm for Asp, 56.2, 562.3 nm for Trp, and 116.4, 645.5 nm for Lys. Despite large aggregates that may be formed at the spot of mixing the stock TPPS and amino acids solutions make a contribution to the intensity-weighted CONTIN results; small ones outnumber large ones as supported by the TEM images (Figure 5). The complex micelles were prepared by adding PEG_{114}-*b*-$P4VP_{61}$ stock solutions immediately after mixing TPPS and amino acids solutions. The diameters are homodispersed, and the average hydrodynamic diameters (D_h) of these corresponding micelles are 104.0, 112.8, and 157.0 nm, close to that of PEG_{114}-*b*-$P4VP_{61}$/TPPS micelles (102.1 nm) and larger than those of small TPPS aggregates, suggesting the occurrence of the micellization. Much bigger size is caused by a few of rodlike micelles in the case of Lys, as proved by the AFM pictures. The parallel experiments were performed on the mixed solutions of copolymer and amino acids without TPPS. DLS results showed weak scattering light intensity and diameter distributions centered at 8−12 nm, which indicated that amino acids did not give rise to a micellization of PEG_{114}-*b*-$P4VP_{61}$.

Figure 1 shows the UV−vis spectra of the TPPS solutions with (spectrum I) and without (spectrum II) Trp in comparison with that of micelle solution (spectrum III) at pH 2. The absorptions of pure TPPS solution at 434 and 645 nm are the typical Soret band and Q-band of the diacid form, respectively. The appearance of sharp and narrow absorption band at 490 nm that are shifted to the red with respect to the monomeric Soret band together with the weak Q-band at 706 nm indicates the formation of J-aggregates. In the presence of Trp, J-aggregation increases proved by the stronger absorption at 490 and 706 nm as shown in spectrum II. Because the Trp molecules are positively charged due to the protonated amino group, they are able to induce aggregation at a higher rate than H^+ alone, which is in accordance with the previous study.[34] As confirmed by our experiment, more basic amino acids lead to intenser aggregation in acidic aqueous solutions. Consequently, the spectrum of TPPS exhibits more sharp absorptions at typical bands of J-aggregates after mixing with Lys which bears two amino groups. On the contrary, Asp acts as an inhibitor that retards the aggregation due to the electrostatic repulsion caused by its excessive carboxyl group. As a result, the intensity of J-aggregates absorptions which are assumed to be caused by the acid condition has no significant differences with that of pure TPPS solution at pH 2.0 (Figure S2). In other words, the more positive charges the amino acid bears, the intenser J-aggregation it causes. The isoelectric point (pI) values for Asp, Trp, and Lys in aqueous solution are 2.77, 5.89, and 9.74; thus, they promoted the formation of J-aggregates in the order of Asp, Trp, and Lys. The introduction of the diblock copolymer PEG_{114}-*b*-$P4VP_{61}$ makes the aggregation

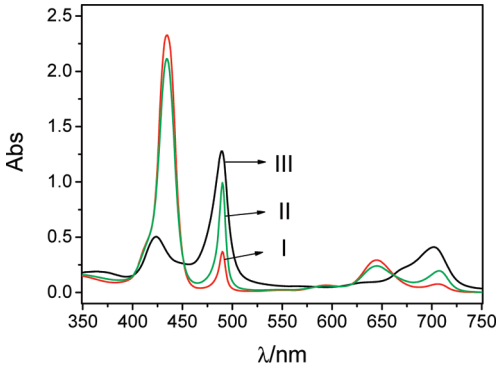

Figure 1. Absorption spectra of the TPPS in the absence (I) and in the presence of Trp (II) and the micelle solution (III) at pH 2, where the PEG_{114}-*b*-$P4VP_{61}$ was added into the solution without any delay time after mixing amino acids and TPPS. TPPS solutions with or without amino acid were measured immediately after preparation. The concentrations of PEG_{114}-*b*-$P4VP_{61}$, TPPS, and Trp were 0.05 g/L, 5 μmol/L, and 5 mmol/L, respectively.

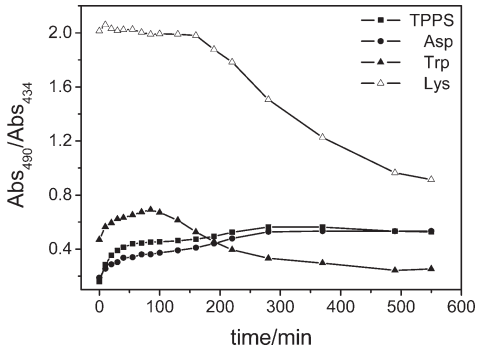

Figure 2. Changes in absorptions of TPPS in the absence (line TPPS) and in the presence of different amino acids (lines Asp, Trp, and Lys) with time. The kinetic profile for the J-aggregation of TPPS was denoted by the ratio of the absorption intensities of 490 nm to 434 nm. The concentrations of TPPS and amino acids were 5 μmol/L and 5 mmol/L, respectively.

reach a stable state where the TPPS is restrained in the core formed by electrostatically complexed TPPS/P4VP that is protected by PEG blocks. Spectrum III takes on a stronger but broader J-aggregation absorption at 490 nm, and the monomer absorption (434 nm) disappears absolutely. The band at 424 nm may be caused by the H-aggregates of TPPS.[25] Similar phenomena occur in the other two systems containing Asp or Lys. The fact that P4VP blocks are able to interact with TPPS in the presence of amino acids demonstrates that the chains of polymer rich in $4VPH^+$ may play an important role in restraining TPPS monomers in a confined region.

Influence of Preservation Time on the Properties of Complex Micelles. The kinetic profiles for the aggregation of TPPS induced by Asp, Trp, and Lys in the absence of PEG_{114}-*b*-$P4VP_{61}$ at pH 2.0 were recorded by the UV−vis spectroscopy and light scattering analysis.

The absorption peak at 490 nm attributed to J-aggregates increases at the expense of the peak at 434 nm due to the monomeric diacid, which indicates that monomers translate into J-aggregates. Thus, the ratio of the absorption intensities of J-aggregates (490 nm) to diacid monomers (434 nm) is used to track the change of the aggregate formation with time as shown in Figure 2. The absorptions were recorded the moment the TPPS stock solution was injected into the amino acids solutions. Rapid growths of the radio are observed in pure TPPS solution and in mixed solution of TPPS and Asp

followed by a mild increase. Finally, it reaches a plateau. The rate of TPPS aggregation in the case of Asp is slower than that of the pure TPPS on account of the retardation effect. An intense aggregation of TPPS presented by the high value of ratio for the Trp and Lys case results from the electrostatic attraction between the protonated amino acid and negatively charged TPPS. The declining stage occurs in Trp and Lys system demonstrates a precipitation formed by large aggregates. However, the ratio value begins to decrease at about 100 min for Trp, earlier than that for Lys. A probable conclusion can be proposed to interpret this result. The large indole group of tryptophan produces a steric hindrance effect on further aggregation of TPPS.

Figure 3 shows the time history plots of the scattered light intensity. The gradually increasing scattered light intensity with time for the pure TPPS indicates the growing size of aggregates interpreting a gradual aggregation process.[36] Asp plays a significant role in prohibiting TPPS from aggregating, which is definitely confirmed by the almost unchanged scattered light intensity with time. As for Trp and Lys, scattered light intensities increase rapidly in the first stage and then reach a plateau, which demonstrates that both Trp and Lys could induce a rapid and marked increase in the aggregates size. The aggregation goes on until the size gets a critical magnitude where precipitation occurs. The fact that the time evolution of the scattered light intensity for Trp system arrives at a relatively stable value earlier than that for Lys is consistent with the results observed in Figure 2. Besides, the strongest scattered light intensity appears in the Lys case, suggesting the largest aggregates among all the experimental TPPS solutions appear in the presence of Lys.

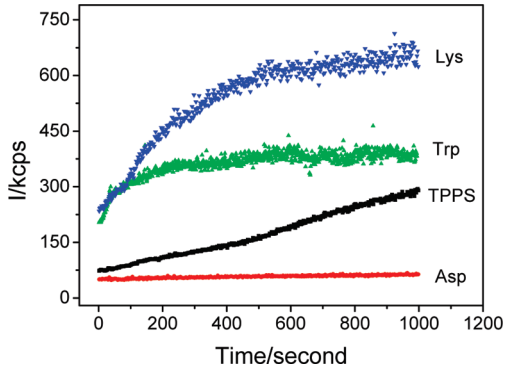

Figure 3. Changes in the scattered light intensity of aggregates of TPPS with time in the absence and in the presence of different amino acids (Asp, Trp, and Lys). The measurements were performed at the scattering angle of 90° at 20 °C. The concentrations of TPPS and amino acids were 5 μmol/L and 5 mmol/L, respectively.

On account of the fact that the three kinds of amino acids have different effects on the process of TPPS aggregation, the time of adding the polymer solution into the TPPS solution with amino acids influenced the spectroscopy properties and morphology of the resulting micellar system. The PEG_{114}-*b*-$P4VP_{61}$ was added after 0, 5, and 15 h preservation time for the mixed solution of TPPS and amino acids to prepare the complex micelles. Figure 4 describes the discrepancy in the absorptions of the resulting micelle solutions. In the case of Asp and Trp (Figure 4, Asp and Trp), there are no evident differences in the spectra of micelle solutions of different preservation time for TPPS and amino acids. On the contrary, for Lys, the latter copolymer is added, and the more intense J-aggregation of TPPS is achieved (Figure 4, Lys). As reported previously, PEG_{114}-*b*-$P4VP_{61}$ is able to cause the J-aggregation of TPPS as well as amino acids.[31] However, PEG_{114}-*b*-$P4VP_{61}$ itself makes the aggregation of TPPS get to a final state soon with the disappearance of monomeric TPPS. Comparing the inducing effects of copolymer and amino acids on the J-aggregation of TPPS, the obtained J-aggregation of TPPS induced by copolymer is much more intense than that induced by Asp, slightly more intense than that induced by Trp, but weaker than that induced by Lys at pH 2.0 (data were not shown). Adding the PEG_{114}-*b*-$P4VP_{61}$ at different time all makes the aggregation of TPPS get to the similar state soon in the case of Asp and Trp. Consequently, absorptions of the complex micelles depend on the concentration of TPPS, the properties of PEG_{114}-*b*-$P4VP_{61}$, and the pH value of the solution and have nothing to do with the preservation time. As for Lys, TPPS undergoes an intense aggregation in the preservation time, leading to the more sharp absorption at 490 nm. Besides, precipitation resulted from large aggregates can be observed in the solution of TPPS in about 2 h for the Trp case and about 1.5 h for Lys, but the solution turned homogeneous again after adding PEG_{114}-*b*-$P4VP_{61}$, which proves that the copolymer plays a key role in stabilizing the aggregated TPPS.

The TEM images show the morphology of the dried TPPS aggregates and the complex micelles in the presence of Trp. In Figure 5/TPPS-a, the diameter distribution of the small aggregates is approximately 30−50 nm. The coexistent larger aggregates may be formed by further interaction between those small ones, which leads to a self-propagation process of TPPS. Thus, the system that underwent several hours' preservation time took on a nanorod appearance (Figure 5/TPPS-b). Figure 5/Micelle-a shows a spherical morphology for the complex micelles with 0 h preservation time. The diameter ranges from 70 to 100 nm, larger than that of small TPPS aggregates. The results come out to be consistent with the obtained DLS data. The micellar system with 15 h

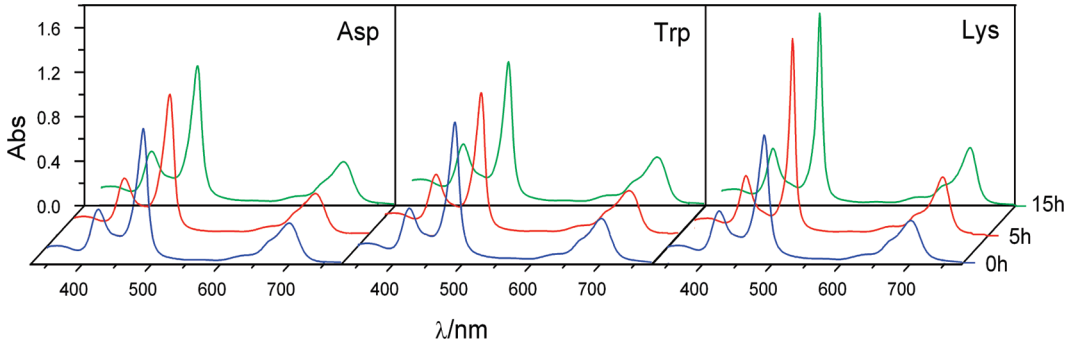

Figure 4. Absorption spectra of the micelle solutions in the presence of different amino acids (Asp, Trp, and Lys) with different preservation time (0, 5, and 15 h) for amino acids and TPPS before adding PEG_{114}-*b*-$P4VP_{61}$. The concentrations of copolymer, TPPS, and amino acids were 0.05 g/L, 5 μmol/L, and 5 mmol/L, respectively.

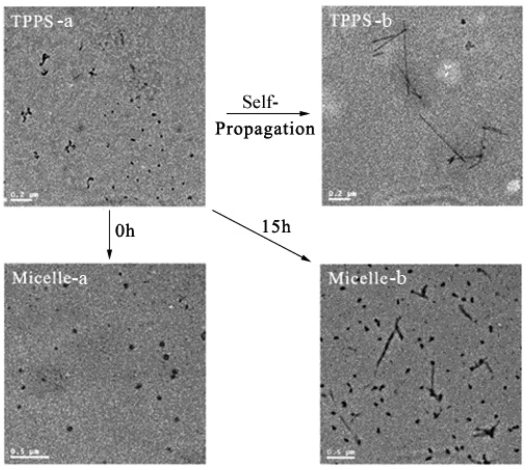

Figure 5. TEM images of the TPPS aggregates and the complex micelles in the presence of amino acid Trp.

preservation time displays the coexistent spherical and rod morphology (Figure 5/Micelle-b).

In the case of Asp and Lys, the results exhibit some differences. The comparison of the morphology of complex micelles in the presence of different amino acids is provided by AFM images (Figure 6). Panels Asp-a, Trp-a, and Lys-a fall into one series, which reveals the morphology of the micelles prepared by adding PEG_{114}-*b*-$P4VP_{61}$ into the solutions immediately after mixing TPPS and amino acids. With the exception that a few rods appear in the case of Lys with a size of about 90 nm in width and 270 nm in length (panel Lys-a), the images in this series show well-defined spheres and the diameter are all in the range of 80−110 nm. The rest of the pictures were ascribed to another series recording the features of the micelles formed by adding PEG_{114}-*b*-$P4VP_{61}$ into the mixed solutions after 15 h preservation for TPPS and amino acids. The morphology of the complex micelles from sphere, short rod (200−500 nm in length) to long rod (300 nm−1.6 μm) in the order of Asp, Trp, and Lys indicates the different influence of amino acids on the aggregation of TPPS according with the results discussed in the kinetics of assembly. Actually, the role of the copolymer is to get a stable assembly state and quench further aggregation of TPPS. It is worth noting that a folding behavior can be observed in the case of Lys (panel Lys-b3). In previous studies,[37,38] straight tapes initially formed by $H_4TPPS_3^-$ evolve to folded particles. However, in our case of H_4TPPS^{2-} the folding structure can be also obtained. The appearance of the folding can be assigned to an entropically driven process.[39] The feature arises from a local and homogeneous interaction with depleting spheres, resulting in a decrease in the free energy gain and an increase in the entropy.

Chirality of the Complex Micelles. Previously, we reported that chiral polymeric micelles can be obtained from achiral TPPS and PEG-*b*-P4VP through adjusting the ratio of protonated pyridyl groups to negatively charged sulfonate residuals or dialyzing the micelle solutions against more acidic water.[30,31] In the presence of chiral molecules, the micelle solutions exhibit strong induced CD spectra in the visible region, as shown in Figure 7. The couplets are due to the TPPS J-aggregates, which show split bands with a crossover at 490 nm. The split bands at 424 nm may be ascribed to H-aggregates of TPPS. It is well-known that induced circular dichroism may appear in aggregates formed by optically inactive molecules.[40] The CD signals derive from the coupling of transition moments of the TPPS molecules as they aggregate. In spite of some differences in the intensity,

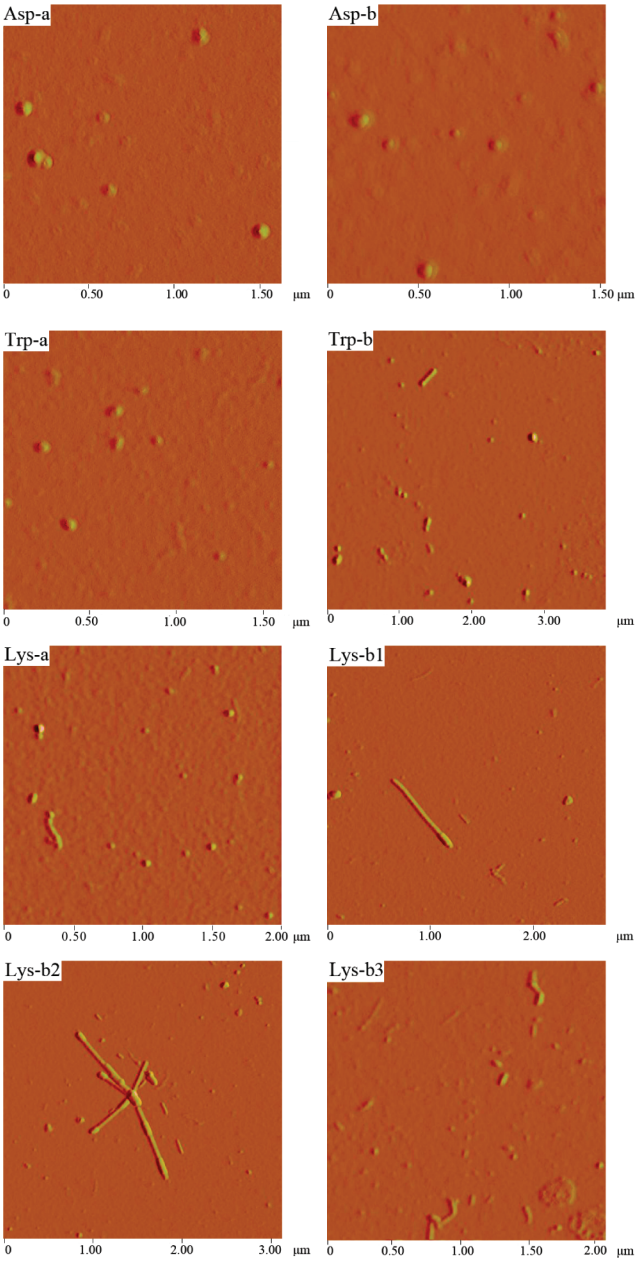

Figure 6. AFM images of the complex micelles in the presence of Asp, Trp, and Lys. *a* and *b* suggest 0 and 15 h preservation time for TPPS and amino acids before adding PEG_{114}-*b*-$P4VP_{61}$. 1, 2, and 3 denote diversified images of the same sample.

according with absorption features for J-aggregation, the Cotton effects for L-Lys and L-Trp are both negative. The chirality signs achieved by L-Lys and L-Trp here are consistent with those reported in the literature.[26,34] However, L-Asp induces a positive sign. The same chirality sign has been obtained in another chiral molecule, L-tartaric acid, which bears two carboxyl groups.[23] For L-Lys and L-Trp, the interaction between amino groups and peripheral sulfonate groups of TPPS leads to a transition moment in the plane of the macrocyclic ring of porphyrin. But the inner protonated nitrogen of TPPS may interact with redundant carboxyl group of Asp via electrostatic or hydrogen bond interaction at pH 2.0. Consequently, the transition moment is not in the plane of, but in a vertical direction to, the macrocyclic ring of porphyrin.[6] As a result, the CD signs for L-Lys/L-Trp and L-Asp are just opposite.

The CD spectra for the L- and D-amino acids are of opposite signs as shown in Figure 8 (only the Trp cases were shown). The increasing intensity of CD signals with the time evolution was also displayed. During the amino acid-induced aggregation process, chiral seeds form first and then promote the formation of the chiral supramolecular aggregates. As a result of an inhibition of the diblock copolymer in further aggregation, the latter polymer was added, and the stronger CD signal was achieved.

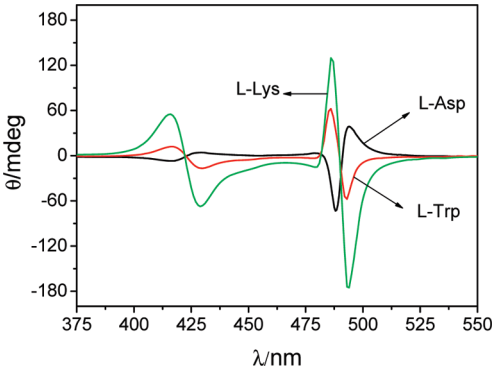

Figure 7. CD spectra for PEG_{114}-*b*-$P4VP_{61}$/TPPS complex micelles in the presence of different amino acids (L-Asp, L-Trp, and L-Lys), where the PEG_{114}-*b*-$P4VP_{61}$ was added into the solution after 15 h preservation for amino acids and TPPS. The concentrations of copolymer, TPPS, and amino acids were 0.05 g/L, 5 μmol/L, and 5 mmol/L, respectively.

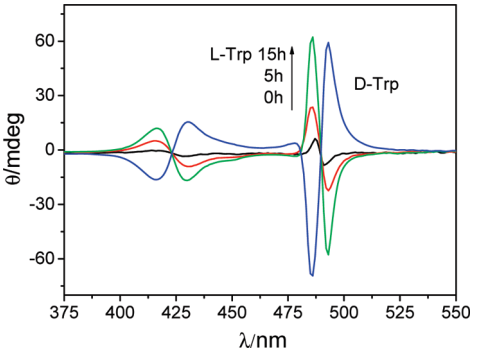

Figure 8. CD spectra for PEG_{114}-*b*-$P4VP_{61}$/TPPS complex micelles in the presence of L- and D-Trp. The arrow suggests an increasing preservation time (0, 5, and 15 h) for amino acids and TPPS before adding PEG_{114}-*b*-$P4VP_{61}$. The concentrations of copolymer, TPPS, and amino acids were 0.05 g/L, 5 μmol/L, and 5 mmol/L, respectively.

It is worth noting that spontaneously formed small J-aggregates of TPPS, which are merely caused by the acid condition, may display a random chirality sign. Such small chiral J-aggregates acting as chiral seeds give rise to the further propagation along their chiral direction. Figure 9 records the results obtained by varying the concentration of L-Trp with a constant concentration of TPPS. The chirality sign shown in Figure 9a is positive and not in accordance with the results shown in Figure 7 that L-Trp leads to a negative Cotton effect. It is supposed that the chiral seeds of the opposite sign form spontaneously and induce a growth in the aggregation, although fewer L-Trp molecules, lacking the quality of guiding the aggregation along their chiral sign, exist in the solution. Higher concentrations of L-Trp make a weaker (Figure 9b) or none (Figure 9c) positive Cotton effect in the initial stage of the aggregation (0 h). Therefore, a certain concentration of amino acids is necessary to offer a chiral environment to direct the Cotton effect sign of aggregated TPPS.

Actually, there are only a thimbleful of L-Trp molecules which may be incorporated into the complex micelles due to interactions between L-Trp and TPPS; most L-Trp molecules stay in the bulk solutions. Because, as mentioned above, the interaction of TPPS with PEG-*b*-P4VP outweighs that with amino acids in micellization and amino acids did not induce micellization of PEG_{114}-*b*-$P4VP_{61}$. On all accounts, Cotton effects are derived from the interaction between amino acids and TPPS, but dissociative chiral molecules that stay in the bulk solutions are also essential for introducing a Cotton effect. This conclusion can also be supported by the fact, indicated by a comparison of the CD intensity in Figure 9, that lower concentration of L-Trp results in weaker CD intensity.

Figure 9 shows the CD spectra obtained by varying the concentration of TPPS with a constant concentration of L-Trp. Obviously, CD intensity increases with increasing the concentration of TPPS. Furthermore, the Cotton effect signs presented by the complex micelles labeled with 15 h are all negative, but positive signs appear at 0 h. The results demonstrate that the Cotton effect sign is reversed from random positive to required negative during preservation in the presence of L-Trp. The concentration of TPPS influences on the rate of reversion. Comparing the Cotton effect signs exhibited by spectral lines labeled with 5 h, the complex micelles with lower concentration of TPPS present negative signs (Figure 10a,b), but those with higher concentration of TPPS still present positive sign (Figure 10c). It is evident that it takes more time to "revise" the aggregates of TPPS from

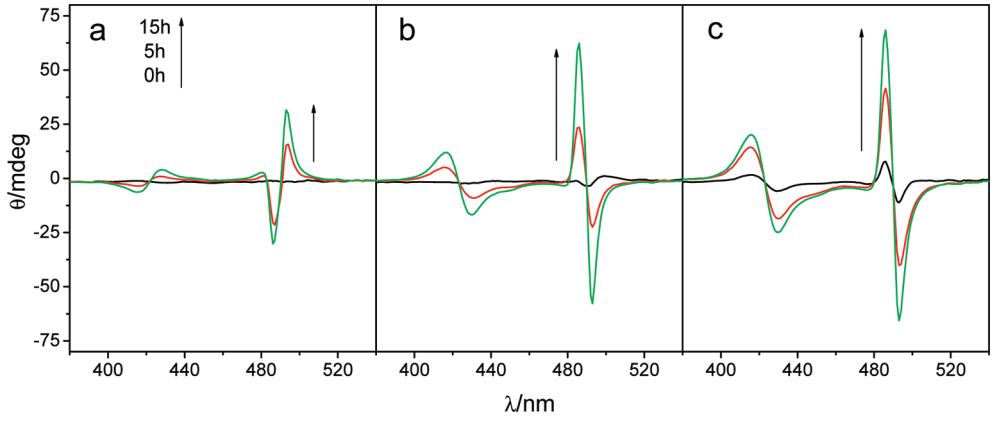

Figure 9. CD spectra for PEG_{114}-*b*-$P4VP_{61}$/TPPS complex micelles in the presence of L-Trp. The arrows suggest an increasing preservation time (0, 5, and 15 h) for amino acids and TPPS before adding PEG_{114}-*b*-$P4VP_{61}$. The concentrations of copolymer and TPPS were 0.05 g/L and 5 μmol/L, respectively. The concentrations of L-Trp were 1 mmol/L (a), 4 mmol/L (b), and 10 mmol/L (c).

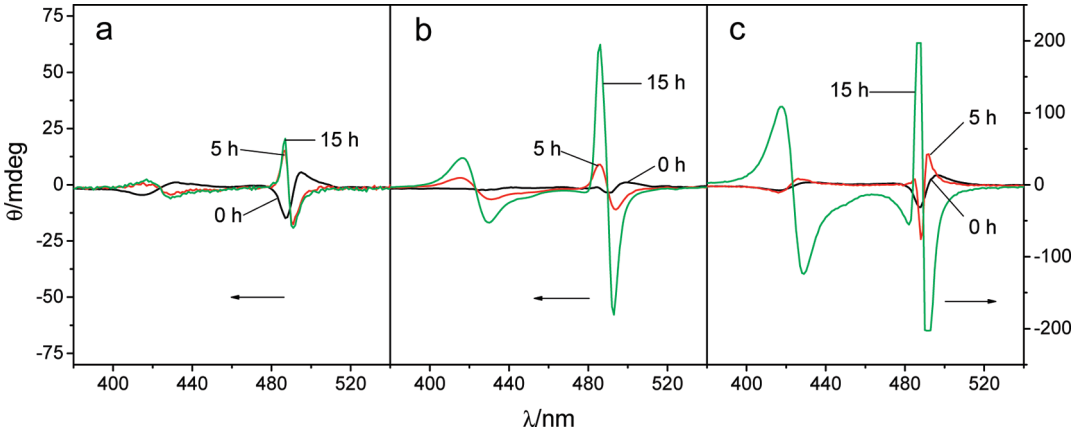

Figure 10. CD spectra for PEG_{114}-*b*-$P4VP_{61}$/TPPS complex micelles in the presence of L-Trp with different preservation time (0, 5, and 15 h) for amino acids and TPPS before adding PEG_{114}-*b*-$P4VP_{61}$. The concentrations of copolymer and L-Trp were 0.05 g/L and 5 mmol/L, respectively. The concentrations of TPPS were 3 μmol/L (a), 5 μmol/L (b), and 10 μmol/L (c).

Scheme 2. Schematic Illustration of the TPPS Monomer-Induced and Aggregate-Induced Micellization of PEG_{114}-*b*-$P4VP_{61}$

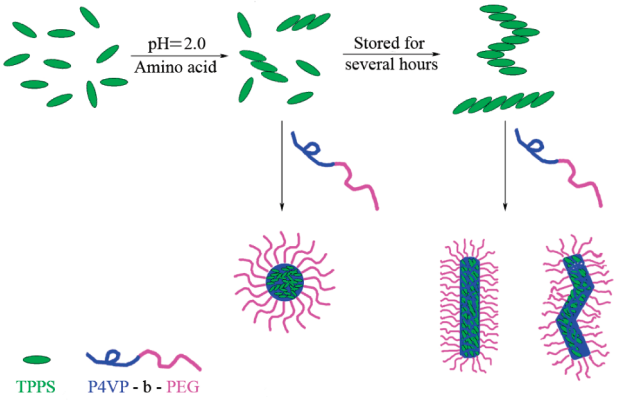

the random positive chirality sign to the required direction at higher concentrations of TPPS. Besides, the increase in the intensity of positive signal displayed by spectrum c-5h in comparison with spectrum c-0h is caused by further propagation from chiral seeds with positive sign.

Scheme 2 illustrates micellization of PEG_{114}-*b*-$P4VP_{61}$ induced by TPPS monomers or aggregates. The aggregation of TPPS increases with time in the presence of amino acids and a certain aging time is needed for the CD appearance. The diblock copolymer not only stabilizes the aggregates but also prohibits the further aggregation. Thus, it is able to catch the intermediate morphology and optical features during the process via its adding at different evolution stages.

Conclusion

The electrostatic interaction between TPPS and P4VP leads to the micellization of copolymer PEG_{114}-*b*-$P4VP_{61}$ in the presence of amino acids at pH 2.0. The properties of small chiral molecules have different effects on the J-aggregation of TPPS. They promoted the formation of J-aggregates in the order of Asp, Trp, and Lys. Aging the TPPS solutions resulted in the morphology evolution of the complex micelles from sphere to rod in the case of Trp and Lys. As for Asp, the spherical appearance remained unchanged. The intensity of the CD signals increases with the preservation time. Furthermore, the chirality of these amino acids determined the chirality sign of the micellar solutions, L-Trp, L-Lys, and D-Asp for a negative chirality sign and the corresponding enantiomers for a positive one. It has been proved that a certain concentration of amino acids was essential to transfer their chiral information to the supramolecular aggregates of TPPS. Lower concentration was not able to "revise" the random chirality sign which appeared in the aggregates spontaneously. Besides, it took a longer time for the aggregates to translate the chirality sign of amino acids at higher concentrations of TPPS. The obtained chiral complex micelles are expected to have the potential applications in chiral separation and asymmetrical catalysis.

Acknowledgment. We thank the National Natural Science Foundation of China (No. 20474032, 20774051), the Program for New Century Excellent Talents in Universities, and the Outstanding Youth Fund (No. 50625310) for financial support.

Supporting Information Available: Hydrodynamic diameter distributions of TPPS aggregates and the corresponding complex micelles in the absense and in the presence of amins acids; absorption spectra of TPPS with and without amino acids. This material is available free of charge via the Internet at http://pubs.acs.org.

References and Notes

(1) Wang, M.; Silva, G. L.; Armitage, B. A. *J. Am. Chem. Soc.* **2000**, *122*, 9977–9986.
(2) Yashima, E.; Maeda, K.; Okamoto, Y. *Nature* (*London*) **1999**, *399*, 449–451.
(3) Oda, R.; Huc, I.; Schmutz, M.; Candau, S. J.; MacKintosh, F. C. *Nature* (*London*) **1999**, *399*, 566–569.
(4) Prins, L. J.; De Jong, F.; Timmerman, P.; Reinhoudt, D. N. *Nature* (*London*) **2000**, *408*, 181–184.
(5) Monti, D.; Venanzi, M.; Stefanelli, M.; Sorrenti, A.; Mancini, G.; Di Natale, C.; Paolesse, R. *J. Am. Chem. Soc.* **2007**, *129*, 6688–6689.
(6) Jiang, S. G.; Liu, M. H. *J. Phys. Chem. B* **2004**, *108*, 2880–2884.
(7) Kondepudi, D. K.; Laudadio, J.; Asakura, K. *J. Am. Chem. Soc.* **1999**, *121*, 1448–1451.
(8) Cornelissen, J.; Rowan, A. E.; Nolte, R. J. M.; Sommerdijk, N. *Chem. Rev.* **2001**, *101*, 4039–4070.
(9) Yashima, E.; Goto, H.; Okamoto, Y. *Macromolecules* **1999**, *32*, 7942–7945.
(10) Yan, Y.; Yu, Z.; Huang, Y. W.; Yuan, W. X.; Wei, Z. X. *Adv. Mater.* **2007**, *19*, 3353–3357.
(11) Kakuchi, R.; Sakai, R.; Otsuka, I.; Satoh, T.; Kaga, H.; Kakuchi, T. *Macromolecules* **2005**, *38*, 9441–9447.
(12) Seo, J. S.; Whang, D.; Lee, H.; Jun, S. I.; Oh, J.; Jeon, Y. J.; Kim, K. *Nature* (*London*) **2000**, *404*, 982–986.
(13) Verbiest, T.; Van Elshocht, S.; Kauranen, M.; Hellemans, L.; Snauwaert, J.; Nuckolls, C.; Katz, T. J.; Persoons, A. *Science* **1998**, *282*, 913–915.
(14) Ogoshi, H.; Mizutani, T. *Acc. Chem. Res.* **1998**, *31*, 81–89.

(15) Furusho, Y.; Kimura, T.; Mizuno, Y.; Aida, T. *J. Am. Chem. Soc.* **1997**, *119*, 5267–5268.
(16) Borovkov, V. V.; Lintuluoto, J. M.; Fujiki, M.; Inoue, Y. *J. Am. Chem. Soc.* **2000**, *122*, 4403–4407.
(17) Kubat, P.; Lang, K.; Janda, P.; Anzenbacher, P. *Langmuir* **2005**, *21*, 9714–9720.
(18) Rosaria, L.; D'Urso, A.; Mammana, A.; Purrello, R. *Chirality* **2008**, *20*, 411–419.
(19) Ribo, J. M.; Crusats, J.; Sague, F.; Claret, J.; Rubires, R. *Science* **2001**, *292*, 2063–2066.
(20) Rubires, R.; Farrera, J. A.; Ribo, J. M. *Chem.—Eur. J.* **2001**, *7*, 436–446.
(21) Zhang, L.; Yuan, J.; Liu, M. H. *J. Phys. Chem. B* **2003**, *107*, 12768–12773.
(22) Zhang, L.; Lu, Q.; Liu, M. H. *J. Phys. Chem. B* **2003**, *107*, 2565–2569.
(23) Ohno, O.; Kaizu, Y.; Kobayashi, H. *J. Chem. Phys.* **1993**, *99*, 4128–4139.
(24) Maiti, N. C.; Mazumdar, S.; Periasamy, N. *J. Phys. Chem. B* **1998**, *102*, 1528–1538.
(25) Akins, D. L.; Zhu, H.-R.; Guo, C. *J. Phys. Chem.* **1994**, *98*, 3612–3618.
(26) Koti, A. S. R.; Periasamy, N. *Chem. Mater.* **2003**, *15*, 369–371.
(27) Kataoka, K.; Harada, A.; Nagasaki, Y. *Adv. Drug Delivery Rev.* **2001**, *47*, 113–131.
(28) Hillmyer, M. A.; Lodge, T. P. *J. Polym. Sci., Part A: Polym. Chem.* **2002**, *40*, 1–8.
(29) Becker, M. L.; Remsen, E. E.; Wooley, K. L. *J. Polym. Sci., Part A: Polym. Chem.* **2001**, *39*, 4152–4166.
(30) Li, J. B.; An, Y. L.; Chen, X.; Xiong, D. A.; Li, Y.; Huang, N.; Shi, L. Q. *Macromol. Rapid Commun.* **2008**, *29*, 214–218.
(31) Zhao, L. Z.; Ma, R. J.; Li, J. B.; Li, Y.; An, Y. L.; Shi, L. Q. *Biomacromolecules* **2008**, *9*, 2601–2608.
(32) Wu, K.; Shi, L. Q.; Zhang, W. Q.; An, Y. L.; Zhang, X.; Li, Z. Y.; Zhu, X. X. *Langmuir* **2006**, *22*, 1474–1477.
(33) Fleischer, E. B.; Palmer, J. M.; Srivastava, T. S.; Chatterjee, A. *J. Am. Chem. Soc.* **1971**, *93*, 3162–3167.
(34) Maiti, N. C.; Mazumdar, S.; Periasamy, N. *J. Phys. Chem. B* **1998**, *102*, 1528–1538.
(35) Sidorov, S. N.; Bronstein, L. M.; Kabachii, Y. A.; Valetsky, P. M.; Soo, P. L.; Maysinger, D.; Eisenberg, A. *Langmuir* **2004**, *20*, 3543–3550.
(36) Micali, N.; Mallamace, F.; Romeo, A.; Purrello, R.; Scolaro, L. M. *J. Phys. Chem. B* **2000**, *104*, 5897–5904.
(37) Escudero, C.; Crusats, J.; Diez-Perez, I.; El-Hachemi, Z.; Ribo, J. M. *Angew. Chem., Int. Ed.* **2006**, *45*, 8032–8035.
(38) Crusats, J.; Claret, J.; Diez-Perez, I.; El-Hachemi, Z.; Garcia-Ortega, H.; Rubires, R.; Sagues, F.; Ribo, J. M. *Chem. Commun.* **2003**, 1588–1589.
(39) Snir, Y.; Kamien, R. D. *Science* **2005**, *307*, 1067–1067.
(40) Pasternack, R. F.; Giannetto, A.; Pagano, P.; Gibbs, E. J. *J. Am. Chem. Soc.* **1991**, *113*, 7799–7800.